DEUTSCHES ELEKTRONEN-SYNCHROTRON

in der HELMHOLTZ-GEMEINSCHAFT

DESY 07-058

May 2007

Theory of Nonlinear Harmonic Generation in Free-Electron Lasers with Helical Wigglers

Gianluca Geloni, Evgeni Saldin, Evgeni Schneidmiller and Mikhail Yurkov

Deutsches Elektronen-Synchrotron DESY, Hamburg

ISSN 0418-9833

NOTKESTRASSE 85 - 22607 HAMBURG

Theory of Nonlinear Harmonic Generation in Free-Electron Lasers with Helical Wigglers

Gianluca Geloni, Evgeni Saldin, Evgeni Schneidmiller and Mikhail Yurkov

Deutsches Elektronen-Synchrotron (DESY), Hamburg, Germany

Abstract

Coherent Harmonic Generation (CHG), and in particular Nonlinear Harmonic Generation (NHG), is of importance for both short wavelength Free-Electron Lasers (FELs), in relation with the achievement of shorter wavelengths with a fixed electron-beam energy, and high-average power FEL resonators, in relation with destructive effects of higher harmonics radiation on mirrors. In this paper we present a treatment of NHG from helical wigglers with particular emphasis on the second harmonic. Our study is based on an exact analytical solution of Maxwell's equations, derived with the help of a Green's function method. In particular, we demonstrate that nonlinear harmonic generation (NHG) from helical wigglers vanishes on axis. Our conclusion is in open contrast with results in literature, that include a kinematical mistake in the description of the electron motion.

Key words: Free-electron Laser (FEL), Nonlinear harmonic generation, Helical wiggler, even harmonics
PACS: 41.60.Cr, 52.59.Rz

1 Introduction

The study of Coherent Harmonic Generation (CHG) is of undisputed relevance in the field of Free-Electron Lasers (FELs). On the one hand, x-ray light sources based on Self-Amplified Spontaneous Emission (SASE) can benefit from CHG to radiate at shorter wavelengths at the same electron beam energy (see e.g. [1]). On the other hand, CHG can be a detrimental effect for high average power FEL oscillators, because of possible mirror damage from harmonics in the ultraviolet [2]. Thus, correct understanding of CHG is of interest for both short wavelengths and high average power applications, that are the two major up-to-date development paths in FEL physics.

CHG is driven by bunching of the electron beam at harmonics of the fundamental, and is characterized by the fact that harmonic components of the bunched beam radiate coherently [3]. The bunching mechanism may be linear or nonlinear. In the first case CHG is named Linear Harmonic Generation (LHG). LHG arises when radiation at a certain harmonic induces electron beam bunching at the same harmonic. In the second case CHG is named Nonlinear Harmonic Generation (NHG). NHG arises when the intensity of the fundamental harmonic [1] is strong enough to induce bunching of electrons at different (higher) harmonics. In FEL processes, harmonic bunching of the electron beam due to interactions with the fundamental is always much stronger than that due to interactions with higher radiation harmonics. As a result only NHG has practical relevance, while LHG can be neglected. In general, CHG can be treated in terms of an electrodynamical problem where Maxwell's equations are solved with given sources in the space-frequency domain. Sources must still be obtained through the solution of self-consistent equations for electrons and fields. However, once these equations are solved one obtains macroscopic current and charge density distributions as a function of transverse and longitudinal coordinates at a given harmonic. Further on, solution of Maxwell's equations with these distributions as given sources characterizes harmonic radiation in the space-frequency domain. The dependence of sources in the space-frequency domain on transverse and longitudinal coordinates is complicated because is the result of the above-mentioned self-consistent process. However, here we deal with an FEL setup where an ultrarelativistic electron beam is sent, in free space, through an undulator with many periods. Then, paraxial and resonance approximation can be applied to simplify the characterization of CHG. In particular, for a fixed transverse position, the longitudinal dependence is always slow on the scale of an undulator period.

[1] Note that this argument is not restricted to the first harmonic. Here we have in mind an FEL lazing at the fundamental.

NHG has been dealt with in the case of a planar wiggler, both theoretically and experimentally, in a number of works [2]-[15]. Odd harmonics have maximal power on axis [2] and are linearly polarized. Even harmonics have been shown to have vanishing on-axis power and to exhibit both horizontal and vertical polarization components.

In this work we present the first exact theory of NHG from helical wigglers. Our treatment is based on an exact solution of Maxwell's equations in the space-frequency domain based on a Green's function technique. In the next Section 2 electromagnetic sources are treated in all generality as given data to be obtained from self-consistent FEL codes. In particular, we will demonstrate that nonlinear harmonic generation (NHG) from helical wigglers vanishes on axis. Later on we will focus on the second harmonic, and discuss a particular study-case. Our results are in contrast with conclusions in [16], where NHG in a helical wiggler has also been addressed and the presence of on-axis power has been reported. In Section 3 we will show that the azimuthal resonance condition introduced in [16] to explain net energy exchange between particles and fields is a misconception. It arises from a kinematical mistake. Namely, the electron rotation angle in the helical wiggler is confused with the azimuthal coordinate of the cylindrical reference system. Consequently, this misconception is passed on to simulations, leading to incorrect results. We conclude our work with some final remarks in Section 4.

2 Theory of nonlinear harmonic generation in helical wigglers

2.1 Complete analysis of the harmonic generation mechanism

In this Section we propose the first exact theory of NHG in helical wigglers. In particular we will give an analysis in the space-frequency domain of the second harmonic generation case.

Paraxial Maxwell's equations in the space-frequency domain can be used to describe radiation from ultra-relativistic electrons (see [17, 18]). Let us call the transverse electric field in the space-frequency domain $\vec{\tilde{E}}_\perp(z, \vec{r}_\perp, \omega)$, where $\vec{r}_\perp = x\vec{e}_x + y\vec{e}_y$ identifies a point on a transverse plane at longitudinal position z, $\vec{e}_x$ and $\vec{e}_y$ being unit vectors in the transverse x and y directions. Here the frequency ω is related to the wavelength λ by $\omega = 2\pi c/\lambda$, c being the speed of light in vacuum. From the paraxial approximation follows that

[2] Here we assume that the bunching wavefront is perpendicular to the (longitudinal) FEL axis.

the electric field envelope $\vec{\tilde{E}}_\perp = \vec{\tilde{E}}_\perp \exp[-i\omega z/c]$ does not vary much along z on the scale of the reduced wavelength $\lambda\!\!\!^{-} = \lambda/(2\pi)$. As a result, the following field equation holds:

$$\mathcal{D}\left[\vec{\tilde{E}}_\perp(z,\vec{r}_\perp,\omega)\right] = \vec{f}(z,\vec{r}_\perp,\omega)\ , \tag{1}$$

where the differential operator $\mathcal{D}$ is defined by

$$\mathcal{D} \equiv \left({\nabla_\perp}^2 + \frac{2i\omega}{c}\frac{\partial}{\partial z}\right)\ , \tag{2}$$

${\nabla_\perp}^2$ being the Laplacian operator over transverse cartesian coordinates. Eq. (1) is Maxwell's equation in paraxial approximation. The source-term vector $\vec{f}(z,\vec{r}_\perp)$ is specified by the trajectory of the source electrons, and can be written in terms of the Fourier transform of the transverse current density, $\vec{\tilde{j}}_\perp(z,\vec{r}_\perp,\omega)$, and of the charge density, $\bar{\rho}(z,\vec{r}_\perp,\omega)$, as

$$\vec{f} = -4\pi\left(\frac{i\omega}{c^2}\vec{\tilde{j}}_\perp - \vec{\nabla}_\perp\bar{\rho}\right)\exp\left[-\frac{i\omega z}{c}\right]\ . \tag{3}$$

In this paper we will treat $\vec{\tilde{j}}_\perp$ and $\bar{\rho}$ as macroscopic quantities, without investigating individual electron contributions. $\vec{\tilde{j}}_\perp$ and $\bar{\rho}$ are regarded as given data, that can be obtained from any FEL code. Codes actually provide the charge density of the modulated electron beam in the time domain $\rho(z,\vec{r}_\perp,t)$. A post-processor can then be used in order to perform the Fourier transform of ρ, that can always be presented as

$$\bar{\rho} = -\widetilde{\rho}(z,\vec{r}_\perp - \vec{r'}_{o\perp}(z),\omega)\exp\left[i\omega\frac{s_o(z)}{v_o}\right]\ , \tag{4}$$

where the minus sign on the right hand side is introduced for notational convenience only. Quantities $\vec{r'}_{o\perp}(z)$, $s_o(z)$ and v_o pertain a reference electron with nominal Lorentz factor γ_o that is injected on axis with no deflection and is guided by the helical undulator field. Such electron follows a helical trajectory $\vec{r'}_{o\perp}(z) = r'_{ox}\vec{e}_x + r'_{oy}\vec{e}_y$. We assume that the reference electron rotates anti-clockwise in the judgement of an observer located after the undulator and looking towards the device, so that

$$r'_{ox}(z) = \frac{K}{\gamma_o k_w}[\cos(k_w z) - 1]\ \ ,\quad r'_{oy}(z) = \frac{K}{\gamma_o k_w}\sin(k_w z)\ . \tag{5}$$

In Eq. (5), $K = \lambda_w e H_w/(2\pi m_e c^2)$ is the undulator parameter, $\lambda_w = 2\pi/k_w$ being the undulator period, $(-e)$ the negative electron charge, H_w the maximal modulus of the undulator magnetic field on-axis, and m_e the rest mass of the electron. The corresponding velocity is described by $\vec{v}_{o\perp}(z) = v_{ox}\vec{e}_x + v_{oy}\vec{e}_y$ with

$$v_{ox}(z) = -\frac{Kc}{\gamma_o}\sin(k_w z) \ , \quad v_{oy}(z) = \ \frac{Kc}{\gamma_o}\cos(k_w z) \ . \tag{6}$$

Finally, $s_o(z)$ is the curvilinear abscissa measured along the trajectory of the reference particle.

One may always present $\bar{\rho}$ as in Eq. (4). However, introduction of $\widetilde{\rho}$ is useful when $\widetilde{\rho}$ is a slowly varying function of z on the wavelength scale. This property is granted by the fact that the charge density distribution under study originates from an FEL process. From this fact it also follows that $\widetilde{\rho}$ is slowly varying on the scale of the undulator period λ_w and is peaked around each harmonic of the fundamental $\omega_r = 2k_w c\bar{\gamma}_z^2$, that is fixed imposing resonance condition between electric field and reference particle. The word "peaked" means that the bandwidth of each harmonic component obeys $\Delta\omega/(h\omega_r) \ll 1$ for each positive integer value h. Here $\bar{\gamma}_z = 1/(1-v_{oz}^2/c^2)$ is the longitudinal Lorentz factor. Note that, for the reference electron, $\bar{\gamma}_z$ does not depend on z. We have

$$\bar{\gamma}_z \equiv \frac{1}{\sqrt{1 - v_{oz}^2/c^2}} = \frac{\gamma}{\sqrt{1+K^2}} \ , \tag{7}$$

where the last equality follows from $v_{oz}^2 = v_o^2 - v_{o\perp}^2$, together with Eq. (6). Finally, the relative deviation of the particles energy from $\gamma_o m_e c^2$ is small, i.e. $\delta\gamma/\gamma_o \ll 1$.

In this paper we will be interested in the case when the transverse beam dimension $\sigma_\perp$ is much larger than the electron rotation radius r_w, i.e. $\sigma_\perp \gg r_w$. We might then substitute the dependence on $\vec{r}_\perp - \vec{r}'_{o\perp}(z)$ in Eq. (4) with a dependence on $\vec{r}_\perp$, because the electron rotation radius is negligible with respect to $\sigma_\perp$ and individual electrons can be considered as occupying a fixed transverse position. However, we will not do so. In fact, starting from Eq. (4) to develop our theory, we will be able to crosscheck our results for an extended source with the well-known asymptotic for a filament beam (see Section 2.2), i.e. $\sigma_\perp \ll r_w$, and demonstrate agreement with results in [20].

We note that for a generic motion one has

$$\omega\left(\frac{s(z_2)-s(z_1)}{v}-\frac{z_2-z_1}{c}\right)=\int_{z_1}^{z_2}d\bar{z}\frac{\omega}{2\gamma_z^2(\bar{z})c}\,, \tag{8}$$

Thus, with the help of Eq. (4), Eq. (3) can be presented as [3]

$$\vec{f}=4\pi\exp\left[i\int_0^z d\bar{z}\frac{\omega}{2\bar{\gamma}_z^2 c}\right]\left[\frac{i\omega}{c^2}\vec{v}_{o\perp}(z)-\vec{\nabla}_\perp\right]\widetilde{\rho}[z;\vec{r}_\perp-\vec{r'}_{o\perp}(z)]\,, \tag{9}$$

where we used the fact that $\vec{\bar{j}}_\perp=\vec{v}_{o\perp}\bar{\rho}$. In fact, for each particle in the beam $\delta\gamma/\gamma_o\ll 1$. Therefore we can neglect differences between the average transverse velocity of electrons $\langle\vec{v}_\perp\rangle$ and $\vec{v}_{o\perp}$, so that $\vec{\bar{j}}_\perp\equiv\langle\vec{v}_\perp\rangle\bar{\rho}\simeq\vec{v}_{o\perp}\bar{\rho}$.

We will now introduce a coherent deflection angle $\vec{\eta}^{(c)}$, where the superscript (c) stands for "coherent", to describe the transverse deflection of the electron beam as a whole [4]. This means that we account for a possible deflection angle $\vec{\eta}^{(c)}$ in the the trajectory of reference electron. We therefore perform the following substitutions in Eq. (9):

$$\begin{aligned}&\vec{r'}_{o\perp}(z)\longrightarrow\vec{r}_\perp^{(c)}(z,\vec{\eta}^{(c)})=\\&\vec{r'}_{o\perp}(z)+\vec{\eta}^{(c)}z=\left\{\frac{K}{\gamma k_w}\left[\cos(k_w z)-1\right]+\eta_x^{(c)}z\right\}\vec{e}_x+\left\{\frac{K}{\gamma k_w}\sin(k_w z)+\eta_y^{(c)}z\right\}\vec{e}_y\,,\end{aligned} \tag{10}$$

$$\begin{aligned}&\vec{v}_{o\perp}(z)\longrightarrow\vec{v}_\perp(z,\vec{\eta}^{(c)})=\\&\vec{v}_{o\perp}(z)+c\vec{\eta}^{(c)}=\left[-\frac{Kc}{\gamma}\sin(k_w z)+c\eta_x^{(c)}\right]\vec{e}_x+\left[\frac{Kc}{\gamma}\cos(k_w z)+c\eta_y^{(c)}\right]\vec{e}_y\,.\end{aligned} \tag{11}$$

Using $\vec{v}_\perp(z,\vec{\eta}^{(c)})$ in place of $\vec{v}_{o\perp}(z)$ implies that $\gamma_z(z,\vec{\eta}^{(c)})$ is now a function of both z and $\vec{\eta}^{(c)}$. In particular, $1/\gamma_z^2(z,\vec{\eta}^{(c)})=1-v_z^2(z,\vec{\eta}^{(c)})/c^2$, where $v_z^2=v^2-v_\perp^2$

[3] Eq. (9) is the analogous of the source term on the right hand side of Eq. (11) in reference [15], dealing with planar undulators and an electron beam modulated at the second harmonic only. There is only a slight notational difference in that the symbol $\widetilde{\rho}$ in the present paper corresponds to $j_o\widetilde{a}_2/c$ in reference [15].

[4] With this, we assume that the deflection angle $\vec{\eta}^{(c)}$ is constant. This is the case only if we do not account for focusing elements within the undulator. Generalization to account for betatron motion of electrons is, however, straightforward.

is the square of the electron longitudinal velocity. It follows that $1/\bar{\gamma}_z^2$ in Eq. (9) should also be substituted according to

$$\frac{1}{\bar{\gamma}_z^2} \longrightarrow \frac{1}{\gamma_z^2(z,\vec{\eta}^{(c)})} = \frac{1}{\bar{\gamma}_z^2} + \left[\left(\eta_x^{(c)}\right)^2 + \left(\eta_y^{(c)}\right)^2\right] + \frac{2K}{\gamma}\left[-\eta_x^{(c)}\sin(k_w z) + \eta_y^{(c)}\cos(k_w z)\right] , \tag{12}$$

yielding

$$\vec{f} = 4\pi \exp\left[i\int_0^z d\bar{z}\frac{\omega}{2c\gamma_z^2(\bar{z},\vec{\eta}^{(c)})}\right]\left[\frac{i\omega}{c^2}\vec{v}_\perp(z,\vec{\eta}^{(c)}) - \vec{\nabla}_\perp\right]\widetilde{\rho}[z;\vec{r}_\perp - \vec{r}_\perp^{(c)}(z,\vec{\eta}^{(c)})] . \tag{13}$$

We find an exact solution of Eq. (2) without any other assumption about the parameters of the problem. A Green's function for Eq. (2), namely the solution corresponding to the unit point source can be written as (see [15]):

$$G(z_o - z'; \vec{r_{\perp o}} - \vec{r'_\perp}) = -\frac{1}{4\pi(z_o - z')}\exp\left\{i\omega\frac{|\vec{r_{\perp o}} - \vec{r'_\perp}|^2}{2c(z_o - z')}\right\} , \tag{14}$$

assuming $z_o - z' > 0$. When $z_o - z' < 0$ the paraxial approximation does not hold, and the paraxial wave equation Eq. (1) should be substituted, in the space-frequency domain, by a more general Helmholtz equation. However, the radiation formation length for $z_o - z' < 0$ is very short with respect to the case $z_o - z' > 0$, i.e. there is no radiation for observer positions $z_o - z' < 0$. As a result, in this paper we will consider only $z_o - z' > 0$. It follows that the observer is located downstream of the sources.

This leads to the solution

$$\vec{\tilde{E}}_\perp(z_o,\vec{r}_{\perp o}) = -\int_{-\infty}^{\infty} dz'\frac{1}{z_o - z'}\int d\vec{r'}_\perp\left[\frac{i\omega}{c^2}\vec{v}_\perp(z',\vec{\eta^{(c)}}) - \vec{\nabla}'_\perp\right] \times\widetilde{\rho}\left(z',\vec{r'}_\perp - \vec{r}_\perp^{(c)}(z',\vec{\eta^{(c)}})\right)\exp\left\{i\omega\left[\frac{|\vec{r}_{\perp o} - \vec{r'}_\perp|^2}{2c(z_o - z')}\right] + i\int_0^{z'} d\bar{z}\frac{\omega}{2c\gamma_z^2(\bar{z},\vec{\eta}^{(c)})}\right\} , \tag{15}$$

where $\vec{\nabla}'_\perp$ represents the gradient operator (acting on transverse coordinates) with respect to the source point, while $(z_o, \vec{r}_{\perp o})$ indicates the observation

point. Note that the integration is taken from $-\infty$ to ∞ because the sources are understood to be localized in a finite region of space (i.e. $\widetilde{\rho}$ is different from zero in a finite region of space). This is in agreement with $z_o - z' > 0$ and within the applicability criteria of the paraxial approximation. Integration by parts of the gradient term leads to

$$\vec{\widetilde{E}}_\perp = -\frac{i\omega}{c}\int_{-\infty}^{\infty} dz' \frac{1}{z_o - z'} \int d\vec{r'}_\perp \left(\frac{\vec{v}_\perp(z', \vec{\eta^{(c)}})}{c} - \frac{\vec{r}_{\perp o} - \vec{r'}_\perp}{z_o - z'} \right) \times \widetilde{\rho}\left(z', \vec{r'}_\perp - \vec{r}^{(c)}_\perp(z', \vec{\eta^{(c)}})\right) \exp\left[i\Phi_T(z', \vec{r'}_\perp, \vec{\eta^{(c)}}) \right] , \tag{16}$$

where the total phase Φ_T is given by

$$\Phi_T = \omega \left[\frac{|\, \vec{r}_{\perp o} - \vec{r'}_\perp\,|^2}{2c(z_o - z')} \right] + \int_0^z d\bar{z} \frac{\omega}{2c\gamma_z^2(\bar{z}, \vec{\eta}^{(c)})} . \tag{17}$$

We now make use of a new integration variable $\vec{l'} = \vec{r'}_\perp - \vec{r}^{(c)}_\perp(z', \vec{\eta^{(c)}})$ so that

$$\vec{\widetilde{E}}_\perp = -\frac{i\omega}{c}\int_{-\infty}^{\infty} dz' \frac{1}{z_o - z'} \int d\vec{l'} \left(\frac{\vec{v}_\perp(z', \vec{\eta^{(c)}})}{c} - \frac{\vec{r}_{\perp o} - \vec{r}^{(c)}_\perp(z', \vec{\eta^{(c)}}) - \vec{l'}}{z_o - z'} \right) \times \widetilde{\rho}\left(z', \vec{l'}\right) \exp\left[i\Phi_T(z', \vec{l'}, \vec{\eta^{(c)}}) \right] , \tag{18}$$

and

$$\Phi_T = \omega \left[\frac{|\vec{r}_{\perp o} - \vec{r}^{(c)}_\perp(z', \vec{\eta^{(c)}}) - \vec{l'}|^2}{2c(z_o - z')} \right] + \int_0^{z'} d\bar{z} \frac{\omega}{2c\gamma_z^2(\bar{z}, \vec{\eta}^{(c)})} . \tag{19}$$

We will be interested in the total power emitted and in the directivity diagram of the radiation in the far zone.

We therefore introduce the far zone approximation calling the observation angle $\vec{\theta} = \vec{r}_{\perp o}/z_o$, setting $\theta \equiv |\vec{\theta}|$ and taking the limit for $z_o \gg L_w$, where $L_w = N_w \lambda_w$ is the undulator length:

$$\vec{\widetilde{E}}_\perp = -\frac{i\omega}{cz_o}\int_{-\infty}^{\infty} dz' \int d\vec{l'} \left(\frac{\vec{v}_\perp(z', \vec{\eta^{(c)}})}{c} - \vec{\theta} \right) \widetilde{\rho}\left(z', \vec{l'}\right)$$

$$\times \exp\left\{\frac{i\omega}{2c}\left[z_o\theta^2 - 2\vec{\theta}\cdot\vec{r}_\perp^{(c)}(z',\vec{\eta^{(c)}}) - 2\vec{\theta}\cdot\vec{l'} + z'\theta^2\right] + i\int_0^{z'} d\bar{z}\frac{\omega}{2c\gamma_z^2(\bar{z},\vec{\eta}^{(c)})}\right\}. \tag{20}$$

Substitution of Eq. (10), Eq. (11) and Eq. (12) in Eq. (20) yields the following field contribution calculated along the undulator:

$$\begin{aligned}\vec{\tilde{E}}_\perp = \frac{i\omega}{cz_o}\int d\vec{l'}\exp\left[i\Phi_o\right]\int_{-L_w/2}^{L_w/2} dz'\widetilde{\rho}\left(z',\vec{l'}\right)\exp\left[i\Phi_T\right] \\ \times\left[\left(\frac{K}{\gamma}\sin\left(k_w z'\right) + \left(\theta_x - \eta_x^{(c)}\right)\right)\vec{e}_x + \left(-\frac{K}{\gamma}\cos\left(k_w z'\right) + \left(\theta_y - \eta_y^{(c)}\right)\right)\vec{e}_y\right]\end{aligned} \tag{21}$$

where

$$\begin{aligned}\Phi_T = \frac{\omega z'}{2c}\left[\frac{1}{\bar{\gamma}_z^2} + \left(\theta_x - \eta_x^{(c)}\right)^2 + \left(\theta_y - \eta_y^{(c)}\right)^2\right] \\ -\frac{K\omega}{c\gamma k_w}\left[\left(\theta_y - \eta_y^{(c)}\right)\sin(k_w z') + \left(\theta_x - \eta_x^{(c)}\right)\cos(k_w z')\right]\end{aligned} \tag{22}$$

and

$$\Phi_o = \frac{\omega}{c}\left[\frac{z_o\left(\theta_x^2 + \theta_y^2\right)}{2} + \frac{K(\theta_x - \eta_x^{(c)})}{k_w\gamma} - (\theta_x l'_x + \theta_y l'_y)\right]. \tag{23}$$

Note that the integration in Eq. (21) is performed in dz' over the undulator length, i.e. is limited to the interval $[-L_w/2, L_w/2]$. The reason for this is that, working under the resonance approximation in the limit for $N_w \gg 1$, one can neglect contributions to the field due to non-resonant elements outside the undulator [18].

We are interested in studying frequency near the fundamental harmonic $\omega_r = 2k_w c\bar{\gamma}_z^2$ or its h-th integer multiple. We specify "how near" the frequency ω is to the h-th harmonic by defining a detuning parameter C_h as

$$C_h = \frac{\omega}{2\bar{\gamma}_z^2 c} - hk_w = \frac{\Delta\omega}{\omega_r}k_w\,. \tag{24}$$

Here $\omega = h\omega_r + \Delta\omega$. Eq. (22) can thus be rewritten as

$$\Phi_T = z'\left[hk_w + C_h + \frac{\omega}{2c}\left(\theta_x - \eta_x^{(c)}\right)^2 + \frac{\omega}{2c}\left(\theta_y - \eta_y^{(c)}\right)^2\right] - \frac{K\omega}{c\gamma k_w}\left[(\theta_y - \eta_y^{(c)})\sin(k_w z') + (\theta_x - \eta_x^{(c)})\cos(k_w z')\right] , \quad (25)$$

so that altogether, Eq. (21) can be presented as:

$$\begin{aligned}\vec{\tilde{E}}_\perp = & \frac{i\omega}{cz_o}\int_{-\infty}^{\infty} dl'_x \int_{-\infty}^{\infty} dl'_y \int_{-L_w/2}^{L_w/2} dz' \widetilde{\rho}\left(z', l'_x, l'_y\right) \\ & \times \exp\left\{i\frac{\omega}{c}\left[\frac{z_o\left(\theta_x^2 + \theta_y^2\right)}{2} + \frac{K\left(\theta_x - \eta_x^{(c)}\right)}{k_w\gamma} - \left(\theta_x l'_x + \theta_y l'_y\right)\right]\right\} \\ & \times \exp\left\{i\left[hk_w + C_h + \frac{\omega}{2c}\left(\theta_x - \eta_x^{(c)}\right)^2 + \frac{\omega}{2c}\left(\theta_y - \eta_y^{(c)}\right)^2\right]z' \right. \\ & \left. -i\frac{K\omega}{c\gamma k_w}\left[(\theta_y - \eta_y^{(c)})\sin(k_w z') + (\theta_x - \eta_x^{(c)})\cos(k_w z')\right]\right\} \\ & \times \left\{\left[\frac{K}{2i\gamma}\left(\exp[ik_w z'] - \exp[-ik_w z']\right) + \left(\theta_x - \eta_x^{(c)}\right)\right]\vec{e}_x \right. \\ & \left. + \left[-\frac{K}{2\gamma}\left(\exp[ik_w z'] + \exp[-ik_w z']\right) + \left(\theta_y - \eta_y^{(c)}\right)\right]\vec{e}_y\right\} , \end{aligned} \quad (26)$$

We make use of the well-known expansion (see [19])

$$\exp\left[ia\sin(\psi)\right] = \sum_{p=-\infty}^{\infty} J_p(a)\exp\left[ip\psi\right] , \quad (27)$$

where J_p indicates the Bessel function of the first kind of order p, while a and ψ are real numbers. Eq. (26) may thus be written as

$$\begin{aligned}\vec{\tilde{E}}_\perp = & \frac{i\omega}{cz_o}\int_{-\infty}^{\infty} dl'_x \int_{-\infty}^{\infty} dl'_y \int_{-L_w/2}^{L_w/2} dz' \widetilde{\rho}\left(z', l'_x, l'_y\right) \\ & \times \exp\left\{i\frac{\omega}{c}\left[\frac{z_o\left(\theta_x^2 + \theta_y^2\right)}{2} + \frac{K(\theta_x - \eta_x^{(c)})}{k_w\gamma} - (\theta_x l'_x + \theta_y l'_y)\right]\right\} \\ & \times \sum_{m,n=-\infty}^{\infty} J_m(u)J_n(v)\exp\left[\frac{i\pi n}{2}\right]\exp\left[i(n+m+h)k_w z'\right] \\ & \times \exp\left\{i\left[C_h + \frac{\omega}{2c}\left(\theta_x - \eta_x^{(c)}\right)^2 + \frac{\omega}{2c}\left(\theta_y - \eta_y^{(c)}\right)^2\right]z'\right\} \\ & \times \left\{\left[\frac{K}{2i\gamma}\left(\exp[ik_w z'] - \exp[-ik_w z']\right) + \left(\theta_x - \eta_x^{(c)}\right)\right]\vec{e}_x\right. \end{aligned}$$

$$+\left[-\frac{K}{2\gamma}\left(\exp[ik_w z'] + \exp[-ik_w z']\right) + \left(\theta_y - \eta_y^{(c)}\right)\right]\vec{e}_y\Bigg\}\ , \tag{28}$$

where

$$u = -\frac{K\omega(\theta_y - \eta_y^{(c)})}{c\gamma k_w} \quad \text{and} \quad v = -\frac{K\omega(\theta_x - \eta_x^{(c)})}{c\gamma k_w}\ . \tag{29}$$

Whenever

$$C_h + \frac{\omega}{2c}\left[\left(\theta_x - \eta_x^{(c)}\right)^2 + \left(\theta_y - \eta_y^{(c)}\right)^2\right] \ll k_w\ , \tag{30}$$

the second phase factor in z' in Eq. (28) (the one containing C_h) is varying slowly on the scale of the undulator period λ_w. As a result, simplifications arise when $N_w \gg 1$, because fast oscillating terms in powers of $\exp[ik_w z']$ effectively average to zero.

Let us use Eq. (28), to discuss harmonic radiation characteristics. Within the resonance approximation we further select frequencies such that

$$\frac{|\Delta\omega|}{\omega_r} \ll 1\ , \quad \text{i.e. } |C_h| \ll k_w\ . \tag{31}$$

Note that this condition on frequencies automatically selects observation angles of interest $h(\vec{\theta} - \vec{\eta}^{(c)})^2 \ll 1/\bar{\gamma}_z^2$. In fact, if one considers observation angles outside this range, condition (30) is not fulfilled, and the integrand in Eq. (28) exhibits fast oscillations on the integration scale L_w. As a result, one obtains zero transverse field, $\vec{E}_\perp = 0$, with accuracy $1/N_w$. Under the constraint imposed by (31), independently of the value of K and for observation angles of interest we have

$$|v| = \left(1 + \frac{\Delta\omega}{h\omega_r}\right)\frac{2K}{\sqrt{1+K^2}}\bar{\gamma}_z h|\theta_x - \eta_x{}^{(c)}| \lesssim \bar{\gamma}_z h|\theta_x - \eta_x{}^{(c)}| \ll 1 \tag{32}$$

and similarly

$$|u| = \left(1 + \frac{\Delta\omega}{h\omega_r}\right)\frac{2K}{\sqrt{1+K^2}}\bar{\gamma}_z h|\theta_y - \eta_y{}^{(c)}| \lesssim \bar{\gamma}_z h|\theta_y - \eta_y{}^{(c)}| \ll 1\ . \tag{33}$$

This means that, independently of K, $|v| \ll 1$ and $|u| \ll 1$, so that we may expand $J_n(v)$ and $J_m(u)$ in Eq. (28) according to $J_p(x) \simeq S^p(p)[2^{-|p|}/\Gamma(1+|p|)]\, x^{|p|}$,

where $S(p)$ gives the sign of the integer p if $p \neq 0$ and unity if $p = 0$, while Γ is the Euler gamma function

$$\Gamma(z) = \int_0^\infty dt\, t^{z-1} \exp[-t]\,. \tag{34}$$

From now on we will restrict our attention to the second harmonic, noting that we may study any harmonic of interest in a similar way.

Thus, $h = 2$. Terms giving a non-zero contribution after integration in dz' in Eq. (28) are those for $n = -m-3$, $n = -m-1$ and $n = -m-2$. Therefore, we rewrite Eq. (28) as:

$$\begin{aligned}
\vec{\tilde{E}}_\perp &= \frac{i\omega}{cz_o} \int_{-\infty}^{\infty} dl'_x \int_{-\infty}^{\infty} dl'_y \int_{-L_w/2}^{L_w/2} dz' \exp\left\{ i\frac{\omega}{c}\left[\frac{z_o\left(\theta_x^2 + \theta_y^2\right)}{2} - \left(\theta_x l'_x + \theta_y l'_y\right)\right]\right\} \\
&\times \widetilde{\rho}\left(z', l'_x, l'_y\right) \exp\left\{ i\left[C_2 + \frac{\omega}{2c}\left(\theta_x - \eta_x^{(c)}\right)^2 + \frac{\omega}{2c}\left(\theta_y - \eta_y^{(c)}\right)^2\right] z'\right\} \\
&\times \sum_{m=-\infty}^{\infty} J_m(u) \exp\left[-\frac{im\pi}{2}\right] \left\{ \left[\frac{K}{2i\gamma}\left(J_{-m-3}(v) \exp\left[-\frac{i3\pi}{2}\right] - J_{-m-1}(v) \exp\left[-\frac{i\pi}{2}\right]\right)\right.\right. \\
&+ \left.\left(\theta_x - \eta_x^{(c)}\right) J_{-m-2}(v) \exp\left[-i\pi\right]\right] \vec{e}_x + \left[-\frac{K}{2\gamma}\left(J_{-m-3}(v) \exp\left[-\frac{3i\pi}{2}\right]\right.\right. \\
&\left.\left.\left. - J_{-m-1}(v) \exp\left[-\frac{i\pi}{2}\right]\right) + \left(\theta_y - \eta_y^{(c)}\right) J_{-m-2}(v) \exp\left[-i\pi\right]\right] \vec{e}_y \right\}\,,
\end{aligned} \tag{35}$$

where we neglected the phase contribution $K(\theta_x - \eta_x^{(c)})/(k_w\gamma)$ because is much smaller than unity. Non-negligible terms in the expansion of $J_p(\cdot)$ are those for small values of $|p|$, because arguments are much smaller than unity.

Let us begin with contributions for $m = 0$. In this case $J_m(u) = J_0(u) \sim 1$ and $J_{-m-1}(v) = J_{-1}(v) \sim v$. Thus, terms in $J_{-m-1}(v)$ scale as Kv/γ. Terms in $J_{-m-3}(v)$ scale as Kv^3/γ and are negligible. Terms in $J_{-m-2}(v)$ scale as $\left|\theta_{x,y} - \eta_{x,y}^{(c)}\right| v^2 \sim 4Kv\bar{\gamma}_z \left|\vec{\theta} - \vec{\eta}^{(c)}\right|^2 / \sqrt{1+K^2} \ll K|v|/\gamma$ and are also negligible.

In the case $m = -1$, $J_m(u) = J_{-1}(u) \sim u$ and $J_{-m-1}(v) = J_0(v) \sim 1$. Thus, terms in $J_{-m-1}(v)$ scale as Ku/γ, that is of the same order of Kv/γ. Terms in $J_{-m-3}(v)$ scale as Kuv^2/γ and are negligible. Terms in $J_{-m-2}(v)$ scale as $\left|\theta_{x,y} - \eta_{x,y}^{(c)}\right| |u|\ |v| \sim 4Ku\bar{\gamma}_z \left|\vec{\theta} - \vec{\eta}^{(c)}\right|^2 / \sqrt{1+K^2} \ll K|u|/\gamma$ and are also negligible.

Similarly, all other values of m give negligible contributions. As a result we

obtain

$$\vec{\tilde{E}}_{\perp} = \frac{i\omega^2\left(\vec{e}_x + i\vec{e}_y\right)}{2cz_o\omega_r}\frac{K^2}{1+K^2}\left[\left(\theta_x - \eta_x^{(c)}\right) + i\left(\theta_y - \eta_y^{(c)}\right)\right]$$
$$\times\int_{-\infty}^{\infty} dl'_x \int_{-\infty}^{\infty} dl'_y \int_{-L_w/2}^{L_w/2} dz' \exp\left\{i\frac{\omega}{c}\left[\frac{z_o\left(\theta_x^2+\theta_y^2\right)}{2} - \left(\theta_x l'_x + \theta_y l'_y\right)\right]\right\}$$
$$\times\widetilde{\rho}\left(z', l'_x, l'_y\right)\exp\left[iC_2 z'\right]\exp\left\{i\frac{\omega}{2c}\left[\left(\theta_x - \eta_x^{(c)}\right)^2 + \left(\theta_y - \eta_y^{(c)}\right)^2\right]z'\right\} . \qquad (36)$$

Note that the electric field is left circularly polarized (rotating anti-clockwise in the judgement of an observer located after the undulator and looking towards the device, as it must be) and vanishes at $\vec{\theta} = \vec{\eta}^{(c)}$. Polarization characteristics are the same as for the fundamental harmonic, although the fundamental does not vanish at $\vec{\theta} = \vec{\eta}^{(c)}$. Spatial resonance is organized along the undulator for particular values of m, as discussed above.

We conclude our analysis of NHG in helical wigglers studying on-axis harmonic generation. We can do so in all generality, i.e. for any harmonic number, with the help of Eq. (28). We set $\vec{\theta} - \vec{\eta}^{(c)} = 0$, because the concept of "on-axis emission" is evidently related to the coherent deflection angle $\vec{\eta}^{(c)}$. We see by inspection that when $\vec{\theta} - \vec{\eta}^{(c)} = 0$, the only non-zero contributions are for $n = m = 0$, because both $u = 0$ and $v = 0$. Thus, Eq. (28) can be rewritten as

$$\vec{\tilde{E}}_{\perp} = \frac{i\omega}{cz_o}\int d\vec{l'}\int_{-L_w/2}^{L_w/2} dz'\widetilde{\rho}\left(z', \vec{l'}\right)\exp\left[iC_h z'\right]$$
$$\times\left\{\left[\frac{K}{2i\gamma}\Big(\exp[i(h+1)k_w z'] - \exp[i(h-1)k_w z']\Big)\right]\vec{e}_x\right.$$
$$\left.+\left[-\frac{K}{2\gamma}\Big(\exp[i(h+1)k_w z'] + \exp[i(h-1)k_w z']\Big)\right]\vec{e}_y\right\} . \qquad (37)$$

Since $\widetilde{\rho}$ is a slowly function of z' on the scale of the undulator period and $C_h \ll k_w$, we see by inspection that, after integration in dz', one obtains non-zero on-axis field only for $h = 1$, leading to

$$\vec{\tilde{E}}_{\perp} = -\frac{K\omega(\vec{x} + i\vec{e}_y)}{2cz_o\gamma}\int d\vec{l'}\int_{-L_w/2}^{L_w/2} dz'\widetilde{\rho}\left(z', \vec{l'}\right)\exp\left[iC_h z'\right] . \qquad (38)$$

All other harmonics vanish on-axis. This result is in open contrast with what

reported in reference [16]. In Section 3 we will elaborate further on this issue.

2.2 *Analysis of a simple model*

Let us treat a particular case to exemplify our results. Namely, let us consider the case when $C_2 = 0$ (i.e. $\omega = 2\omega_r$) and $\widetilde{\rho}\left(z', l'_x, l'_y\right)$ is given by

$$\widetilde{\rho} = \frac{I_o a_2}{2\pi c \sigma_\perp^2} \exp\left(-\frac{l'^2_x + l'^2_y}{2\sigma_\perp^2}\right) \exp\left[i\frac{2\omega_r}{c}\left(\eta_x^{(c)} l'_x + \eta_y^{(c)} l'_y\right)\right] H_{L_w}(z)\,, \tag{39}$$

with H_{L_w} a window function equal unity inside the undulator and zero everywhere else. Here I_o is the bunch current, a_2 is a constant determining the strength of the bunching and $\sigma_\perp$ the rms transverse size of the electron beam.

This particular case corresponds to a modulation wavefront perpendicular to the direction of motion of the beam [5] . In this case Eq. (36) can be written as

$$\begin{aligned}\vec{\widetilde{E}}_\perp = {} & \frac{i\omega_r I_o a_2 \left(\vec{e}_x + i\vec{e}_y\right)}{\pi\sigma_\perp^2 c^2 z_o} \frac{K^2}{1+K^2}\left[\left(\theta_x - \eta_x^{(c)}\right) + i\left(\theta_y - \eta_y^{(c)}\right)\right] \exp\left[i\frac{\omega_r}{c} z_o(\theta_x^2 + \theta_y^2)\right] \\ & \times \int_{-\infty}^{\infty} dl'_x \int_{-\infty}^{\infty} dl'_y \int_{-\infty}^{\infty} dz' \exp\left\{-i\frac{2\omega_r}{c}\left[\left(\theta_x - \eta_x^{(c)}\right) l'_x + \left(\theta_y - \eta_y^{(c)}\right) l'_y\right]\right\} H_{L_w}(z') \\ & \times \exp\left\{i\frac{\omega_r}{c}\left[\left(\theta_x - \eta_x^{(c)}\right)^2 + \left(\theta_y - \eta_y^{(c)}\right)^2\right] z'\right\} \exp\left(-\frac{l'^2_x + l'^2_y}{2\sigma_\perp^2}\right).\end{aligned} \tag{40}$$

Direct calculations yield

[5] Information about the modulation wavefront of the beam is included in $\widetilde{\rho}$. A phase factor of the form $\exp\left[i\omega\alpha\, \vec{\eta^{(c)}} \cdot \vec{l'}/c\right]$ describes a plane wavefront. The case $\alpha = 1$ that is considered here corresponds to a modulation wavefront orthogonal to the z axis. When $\alpha = 0$ the modulation wavefront is orthogonal to the direction of propagation. Other values correspond to a modulation wavefront that is orthogonal *neither* to the z axis *nor* to the direction of propagation. This may be the case in SASE XFEL setups with very long saturation lengths (order of 10^2 m), where there can be coherent orbit perturbations. Note that if the beam is prepared in a different way so that, for instance, the modulation wavefront is not orthogonal to the direction of propagation of the beam, Eq. (36) retains its validity.

$$\vec{\tilde{E}}_{\perp} = \frac{2iI_o a_2 L_w \omega_r \left(\vec{e}_x + i\vec{e}_y\right)}{c^2 z_o}\left(\frac{K^2}{1+K^2}\right)\left[\left(\theta_x - \eta_x^{(c)}\right) + i\left(\theta_y - \eta_y^{(c)}\right)\right]$$
$$\times \exp\left[i\frac{\omega_r}{c} z_o(\theta_x^2 + \theta_y^2)\right] \exp\left\{-\frac{2\sigma_\perp^2 \omega_r^2}{c^2}\left[\left(\theta_x - \eta_x^{(c)}\right)^2 + \left(\theta_y - \eta_y^{(c)}\right)^2\right]\right\}$$
$$\times \mathrm{sinc}\left\{\frac{L_w \omega_r}{2c}\left[\left(\theta_x - \eta_x^{(c)}\right)^2 + \left(\theta_y - \eta_y^{(c)}\right)^2\right]\right\} . \tag{41}$$

Going back to our particular case in Eq. (41), a subject of particular interest is the angular distribution of the radiation intensity, which will be denoted with I_2. Upon introduction of normalized quantities

$$\hat{\theta}_{x,y} = \sqrt{\frac{2\omega_r L_w}{c}}\,\theta_{x,y} = \sqrt{8\pi N_w}\,\bar{\gamma}_z\,\theta_{x,y}$$
$$\hat{\eta}_{x,y}^{(c)} = \sqrt{\frac{2\omega_r L_w}{c}}\,\eta_{x,y}^{(c)} = \sqrt{8\pi N_w}\,\bar{\gamma}_z\,\eta_{x,y}^{(c)} \tag{42}$$

and of the Fresnel number

$$N = \frac{2\omega_r \sigma_\perp^2}{c L_w} , \tag{43}$$

one obtains

$$I_2\left(\left|\vec{\hat{\theta}} - \vec{\hat{\eta}}^{(c)}\right|\right) = \mathrm{const} \times \left|\vec{\hat{\theta}} - \vec{\hat{\eta}}^{(c)}\right|^2 \exp\left\{-N\left|\vec{\hat{\theta}} - \vec{\hat{\eta}}^{(c)}\right|^2\right\} \mathrm{sinc}^2\left\{\frac{1}{4}\left|\vec{\hat{\theta}} - \vec{\hat{\eta}}^{(c)}\right|^2\right\} . \tag{44}$$

In the limit for $N \ll 1$, Eq. (44) gives back the directivity diagram for the second harmonic radiation from a single particle in agreement with [20].

As an example, the directivity diagram in Eq. (44) is plotted in Fig. 1 for different values of N as a function of $\left|\vec{\hat{\theta}} - \vec{\hat{\eta}}^{(c)}\right|$, normalized to the maximal intensity $I_2^{\max}$ at each value of N.

The next step is the calculation of the second harmonic power that is given by

$$W_2 = \frac{c}{4\pi}\int_{-\infty}^{\infty} dx_o \int_{-\infty}^{\infty} dy_o \overline{|\vec{E}_\perp(z_o, x_o, y_o, t)|^2} = \frac{c}{2\pi}\int_{-\infty}^{\infty} dx_o \int_{-\infty}^{\infty} dy_o |\vec{\tilde{E}}_\perp(z_o, x_o, y_o)|^2 , \tag{45}$$

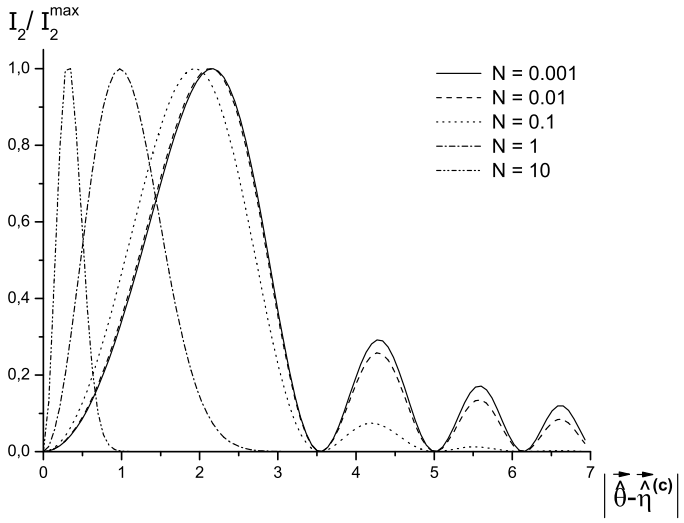

Fig. 1. Plot of the directivity diagram for the radiation intensity as a function of $\left|\vec{\hat{\theta}} - \vec{\hat{\eta}}^{(c)}\right|$ for different values of N, normalized to the maximal intensity $I_2^{\max}$ at each value of N.

where $\overline{(...)}$ denotes averaging over a cycle of oscillation of the carrier wave and $\vec{E}_\perp(z_o, x_o, y_o, t)$ is the electric field in the space-time domain at position (x_o, y_o, z_o) and time t .

We will still consider the model specified by Eq. (39) with $C_2 = 0$. It is convenient to present the expressions for W_2 in a dimensionless form. After appropriate normalization it is a function of one dimensionless parameter only, that is

$$\hat{W}_2 = F_2(N) = \ln\left(1 + \frac{1}{4N^2}\right). \tag{46}$$

Here $\hat{W}_2 = W_2/W_o^{(2)}$ is the normalized power, while the normalization constant $W_o^{(2)}$ is given by

$$W_o^{(2)} = \left(\frac{2K^2}{1+K^2}\right)^2 \frac{I_o^2}{c} a_2^2 \,. \tag{47}$$

For practical purposes it is convenient to express Eq. (47) in the form

$$W_o^{(2)} = \left(\frac{2K^2}{1+K^2}\right)^2 W_b a_2^2 \left(\frac{I_o}{\gamma I_A}\right), \tag{48}$$

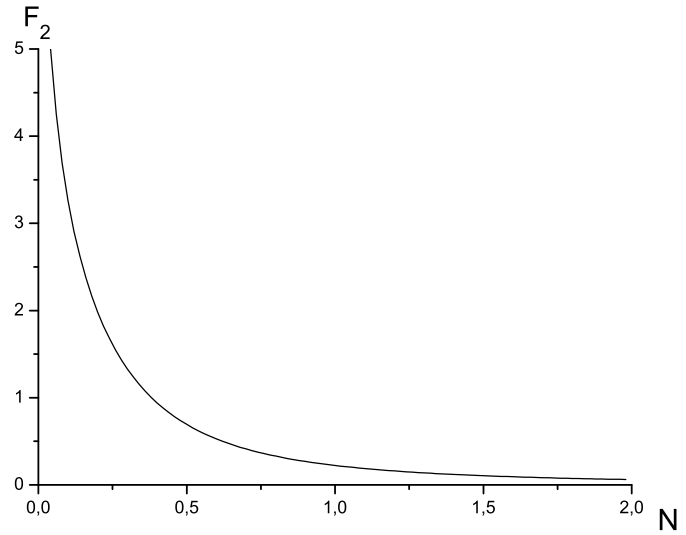

Fig. 2. Illustration of the behavior of $F_2(N)$.

where $W_b = m_e c^2 \gamma I_o / e$ is the total power of the electron beam and $I_A = m_e c^3 / e \simeq 17$ kA is the Alfven current.

The function $F_2(N)$ is plotted in Fig. 2. The logarithmic divergence in $F_2(N)$ in the limit for $N \ll 1$ imposes a limit on the meaningful values of N. On the one hand, the characteristic angle $\hat{\theta}_{\max}$ associated with the intensity distribution is given by $\hat{\theta}^2_{\max} \sim 1/N$. On the other hand, the expansion of the Bessel function performed in Eq. (36) is valid only as $\hat{\theta}^2 \lesssim N_w$. As a result we find that Eq. (46) is valid only up to values of N such that $N \gtrsim N_w^{-1}$. However, in the case $N < N_w^{-1}$ we deal with a situation where the dimensionless problem parameter N is smaller than the accuracy of the resonance approximation $\sim N_w^{-1}$. In this situation our electrodynamic description does not distinguish anymore between a beam with finite transverse size and a point-like particle and, for estimations, we should replace $\ln(N)$ with $\ln(N_w^{-1})$.

3 Discussion

NHG in a helical wiggler has been addressed in [16]. In the numerical study-case proposed in that reference, an ultrarelativistic beam at 140 MeV is considered, driving an FEL oscillator operating near 1 μm wavelength in free space. NHG is studied through simulations for an undulator with a uniform field region of 20 periods. The complete parameter set can be found in reference [16]. For our purpose, parameters reported above are enough to guarantee that paraxial and resonance approximation can be applied to

the study-case in [16]. In that reference one can read: "Our conjecture was that on-axis harmonic excitation due to NHG in helical wigglers can arise because the nonlinear bunching due to the fundamental creates on-axis harmonic radiation. This conjecture is borne out in simulation", and also: "Because NHG is driven by the fundamental, which excites on-axis modes, we speculate that NHG in helical wigglers will have substantial on-axis power". In the same reference one finds a statement regarding harmonic radiation from a single electron too: "Kincaid [20] showed that spontaneous generation from helical wigglers vanishes on axis".

Thus, the main result of [16] is that characteristics of helical undulator radiation from an extended source, i.e. a bunched electron beam, are drastically different compared to those from a single electron studied in [20]. In the previous Section we have seen that our conclusions are in open contrast to [16]. In this Section we give reasons why, in our understanding, results in [16] are incorrect.

A first hint follows from general properties of linear superposition. Any linear superposition of a given field harmonic from single electrons conserves single-particle characteristics like parametric dependence on undulator parameters and polarization. In particular, if a field harmonic from a single electron vanishes on-axis, it must vanish for the linear superposition as well. Consider a bunched beam prepared in such a way that electrons enter the undulator with fixed offsets with respect to the longitudinal axis and with specific phases related with their positions along the bunch. Radiation fields generated by this beam can be seen as a linear superposition of fields from individual electrons. Now, as shown in [20], harmonic radiation from each of these electrons vanishes on axis. It follows that the total field has zero on-axis power as well. This property is conserved when the dependence of charge and current density distributions of the sources on the longitudinal coordinate is slow on the scale of the undulator period. This is always the case for NHG from ultrarelativistic beams in an FEL system in free space.

This argument suggests that results in reference [16] are incorrect. A formal demonstration of this fact can be given discussing the mechanism proposed in [16] to explain net energy exchange between individual electrons and harmonics of the fundamental in helical undulators. This is obtained through an azimuthal resonance condition, that is introduced with these words [6]: "The azimuthal electron motion in helical wigglers is $\theta = k_w z$ (k_w is the wave number for the wiggler period λ_w), which couples to circularly polarized waves that vary as $\exp(i\phi_h)$, where $\phi_h = kz + h\theta - \omega t$ is the wave phase.

[6] Note that this mechanism is independent of the type of harmonic generation process, because it involves interaction between a single particle and the electromagnetic field. In particular, it pertains both LHG and NHG.

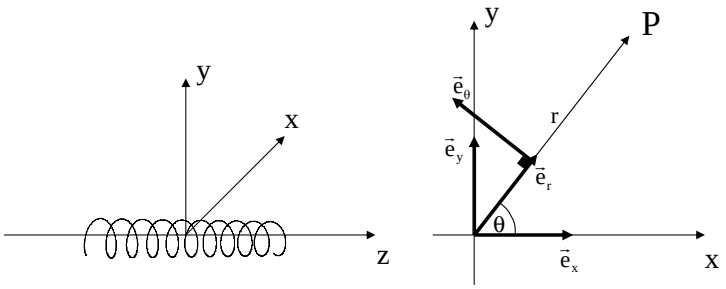

Fig. 3. Cylindrical coordinate system and undulator setup.

Hence, the phase along the particle trajectories varies as $\phi_h = (k + hk_w)z - \omega t$, and the hth order azimuthal mode corresponds to the hth harmonic resonance [i.e., $\omega \approx (k + hk_w)v_z$]" (cited from [16]). Here θ indicates an azimuthal position as in Fig. 3.

It should be remarked that for $h = 1$ one obtains $\omega \approx (k + k_w)v_z$ that is the usual resonance condition between an azimuthal symmetric wave and an electron in a helical undulator. This means that the phase $\phi_h = kz + h\theta - \omega t$ pertains a circularly polarized wave whose electric field is written in terms of unit vectors $\vec{e}_\rho$ and $\vec{e}_\theta$ in polar coordinates, and not in terms of unit vectors $\vec{e}_x$ and $\vec{e}_y$ in cartesian coordinates ($\vec{e}_\rho$, $\vec{e}_\theta$, $\vec{e}_x$ and $\vec{e}_y$ are defined in Fig. 3). In fact one may write the electric field of a (e.g. left) circularly polarized plane wave at position $\vec{r}$ and time t as :

$$\begin{aligned}\vec{E}\left(\vec{r},t\right) &= E_o\left(\vec{e}_x + i\,\vec{e}_y\right)\exp\left[ikz + i(h-1)\theta - i\omega t\right] \\ &= E_o\left(\vec{e}_r + i\,\vec{e}_\theta\right)\exp\left[ikz + ih\theta - i\omega t\right] \equiv E_o\left(\vec{e}_r + i\,\vec{e}_\theta\right)\exp\left[i\phi_h\right], \qquad (49)\end{aligned}$$

E_o being a constant field strength. This definition of ϕ_h is in agreement with notation in [21, 22], and justify words in [16]: "the hth order azimuthal mode corresponds to the hth harmonic resonance". In fact, we can write the angle ψ between the transverse velocity of the electron and the transverse electric field vector as $\psi = k_w z + [kz + (h-1)\theta - \omega t]$. Authors of [16, 21] use relation $\theta \approx k_w z$ in the expression for ϕ_h, and automatically in the expression for ψ too. Using also $dz = v_z dt$, where $v_z \simeq c$ is constant for an electron in a helical undulator, they obtain resonance for $d\psi/(dz) = k + hk_w - \omega/v_z = 0$. As said before, for the particular case $h = 1$ (fundamental harmonic) one has $h - 1 = 0$ (azimuthal-symmetric wave) and $d\psi/(dz) = 0$ for $\omega = (k + k_w)v_z$, that is the usual resonance condition.

We argue that the azimuthal resonance described above is a misconception arising from a kinematical mistake. Namely, it is incorrect to use relation $\theta \approx k_w z$ in the expression for ψ as done in [16, 21]. Let us show this fact.

We begin introducing some characteristic scale of interest. On the one hand,

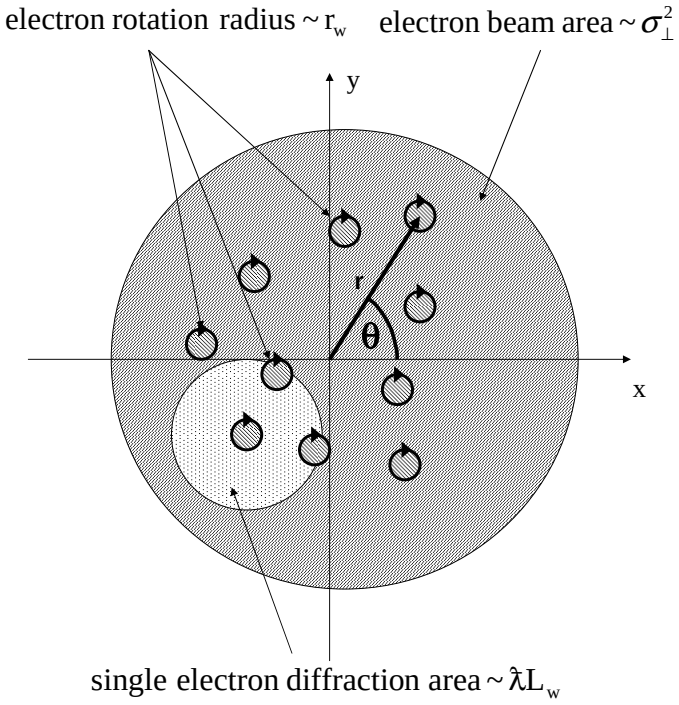

Fig. 4. Hierarchy of characteristic scales of interest.

the radiation diffraction size for a single particle is of order $\sqrt{ƛL_w}$. On the other hand, the electron rotation radius is given by $r_w = (K/\gamma)ƛ_w$. It follows that

$$\frac{r_w^2}{ƛL_w} = \frac{1}{ƛL_w}\frac{K^2}{\gamma^2}ƛ_w^2 = \frac{1}{ƛL_w}\frac{2K^2}{1+K^2}ƛƛ_w = \frac{K^2}{\pi N_w(1+K^2)} \ll 1\,, \tag{50}$$

where we used the fact that $\gamma^2 = (1+K^2)\bar{\gamma}_z^2$, where $\bar{\gamma}_z$ has been introduced in Eq. (7). Inequality (50) holds independently of the value of K, because $N_w \gg 1$. Thus, the electron rotation radius is always much smaller than the radiation diffraction size. To complete the picture we introduce a last characteristic scale of interest in our problem, pertaining the electron beam rather than a single electron. This scale is the transverse size of the electron beam, $\sigma_\perp$. Straightforward geometrical considerations show that it makes sense to talk about $\sigma_\perp$ only when $\sigma_\perp^2 \gg r_w^2$. This is the case in practical situations of interest. There is still room to compare the beam size $\sigma_\perp$ with the radiation diffraction size. In the case $\sigma_\perp \ll \sqrt{ƛL_w}$ we deal with a filament electron beam, and results in [20] can be directly applied. In the opposite case the filament beam approximation breaks down. We are interested in this last case, where single-particle results cannot be used. We have therefore

established a hierarchy in the characteristic scales of interest: $\sigma_\perp^2 \gtrsim \lambda L_w \gg r_w^2$. The situation is described in Fig. 4, where we schematically indicated the electron beam area and the diffraction area as disks. In Fig. 4 we also indicate the azimuthal and radial coordinates of a single electron, respectively θ and r. As one can see, the azimuthal coordinate of each electron, θ, is fixed during the motion inside the undulator with the accuracy of the resonance approximation, scaling as $1/N_w$. In contrast to this, the identification $\theta \approx k_w z$ is made in [16, 21]. This is a kinematical mistake. If $\theta \approx k_w z$ each electron would be rotating around the origin of the coordinate system, that is not the case. Thus, we have shown that $\psi = k_w z + [kz + (h-1)\theta - \omega t]$ with θ constant for each electron along the trajectory in the undulator. As a result $d\psi/(dz) = 0$ only for $h = 1$ that yields the usual resonance condition $\omega = (k + k_w)v_z$. Summing up, our conclusion is that a kinematical mistake is at the origin of the azimuthal resonance described in [16, 21]. The azimuthal resonance condition is a misconception following from this mistake. This misconception is subsequently passed on to simulations in [16], resulting in incorrect outcomes. Harmonic emission exists for a single electron [20], and it also exists for an electron bunch. However, qualitative properties are different with respect to what has been predicted in [16]. In particular, as we have seen in Section 2, on-axis power vanishes.

4 Conclusions

In this paper we discussed NHG in helical undulators, with particular emphasis on second harmonic generation. First we discussed the NHG mechanism in helical undulators in all generality. Then we specialized our study to the case of second harmonic generation. Finally, to exemplify our results, we treated a simplified model where the beam modulation wavefront is orthogonal to the z axis, has a Gaussian transverse profile and is independent on the position inside the undulator.

Our results show that on-axis harmonic generation from helical wigglers vanishes. This applies to any harmonic of interest with the exclusion of the fundamental, and independently of the form of the electron beam modulation (assuming that the electron beam as a whole propagates on-axis). Important consequences follow regarding the two mainstream development paths in FEL physics. First, as concerns short wavelength (x-ray) SASE FEL devices, vanishing on-axis harmonics make the option of a helical undulator less attractive as regards the exploitation of NHG radiation. Second, as concerns high average-power FEL oscillators, vanishing on-axis harmonics suggest that helical undulators carry relevant advantages over planar undulators, as potential for mirror damage is reduced.

Previous studies reported non-vanishing on-axis power, due to the nature of a particular azimuthal resonance condition. We showed that this resonance condition is a misconception, arising from a kinematical mistake. This misconception was passed on to simulations, that confirmed the presence of on-axis power out of NHG from helical wigglers. This result is also incorrect. Simulations are undoubtedly very important scientific tools, but they follow specific models. The correctness of their outcomes is related to the correctness of these models, meaning that validity of simulations should always be cross-checked with analytical results from simplified study-cases.

5 Acknowledgements

We thank Martin Dohlus (DESY) for useful discussions, Massimo Altarelli (DESY) and Jochen Schneider (DESY) for their interest in this work.

References

[1] M. Altarelli et al. (Eds.), XFEL: The European X-Ray Free-Electron Laser. Technical Design Report, DESY 2006-097, DESY, Hamburg (2006) (See also http://xfel.desy.de)

[2] H.P. Freund, P.G. O'Shea and S.G. Biedron, Nucl. Instrum. Methods Phys. Res. A 528, 44 (2004)

[3] Z. Huang and K.-Je Kim, Phys. Rev. E, 62, 7295 (2000)

[4] M. Schmitt and C. Elliot, Phys. Rev. A 34 (1986)

[5] R. Bonifacio, L. De Salvo, and P. Pierini, Nucl. Instrum. and Methods A 293, 627 (1990)

[6] W.M. Fawley et al., "Large harmonic bunching in a high-gain free-electron laser", Proc. IEEE Part. Acc. Conf., 219 (1995)

[7] H. Freund, S. Biedron and S. Milton, Nucl. Instrum. and Methods A 445 (2000)

[8] H. Freund, S. Biedron and S. Milton, IEEE J. Quant. Electr. 36, 275 (2000)

[9] S. Biedron et al., Nucl. Instrum. and Methods A 483, 94 (2002)

[10] S. Biedron et al., Phys. Rev. ST 5 (2002) 030701.

[11] Z. Huang and K. Kim, Nucl. Instrum. and Methods A 475, 112 (2001)

[12] A. Tremaine et al., Phys. Rev. Lett. 88 (2002) 204801.

[13] W. Brefeld et al., Nucl. Instrum. and Methods A 507, 431 (2003)

[14] E.L. Saldin, E.A. Schneidmiller and M.V. Yurkov, Phys. Rev. ST 9(2006) 030702.

[15] G. Geloni, E. Saldin, E. Schneidmiller and M. Yurkov, Opt. Comm., 271, 1, 207 (2007)

[16] H.P. Freund, P.G. O'Shea and S.G. Biedron, Physical Review Letters, 94, 074802 (2005)

[17] G. Geloni, E. Saldin, E. Schneidmiller and M. Yurkov, "Fourier Optics Treatment of Classical Relativistic Electrodynamics", DESY 06-127 (2006)

[18] G. Geloni, E. Saldin, E. Schneidmiller and M. Yurkov, "Undulator Radiation in a Waveguide", DESY 07-031 (2007)

[19] D. Alferov, Y. Bashmakov and E. Bessonov, Sov. phys. - Tech. Phys. 18, 1336 (1974)

[20] B. Kinkcaid, J. Appl. Phys, 48, 7, 2684 (1977)

[21] H.P. Freund and T.M. Antonsen, Jr., "Principles of Free-Electron Lasers", Chapman and Hall, London (1996), Chap. 7

[22] A.K. Ganguly and H.P. Freund, Phys. Rev. A, 32, 2275 (1985)